

Supporting Information

Low-valence Bicomponent $(\text{FeO})_x(\text{MnO})_{1-x}$ Nanocrystals Embedded in Amorphous Carbon as High-Performance Anode Materials for Lithium Storage

Guiqiang Diao,^a Muhammad-Sadeeq Balogun,^{*b} Si-Yao Tong,^f Xianzi Guo,^a Xue Huang,^c

Yanchao Mao,^e and Yexiang Tong^{*d}

^aSchool of Chemistry and Materials Engineering, Huizhou University, 516007 Huizhou, PR China..

^bCollege of Materials Science and Engineering, Hunan University, Changsha, 410012 P. R. China. *E-mail: balogun@hnu.edu.cn

^cCollege of Chemistry and Chemical Engineering, Zhongkai University of Agriculture and Engineering, Guangzhou, 510225, China.

^dMOE of the Key Laboratory of Bioinorganic and Synthetic Chemistry, KLGHEI of Environment and Energy Chemistry, School of Chemistry, Sun Yat-Sen University, Guangzhou 510275 P. R. China *E-mail: chedhx@mail.sysu.edu.cn

^eMOE Key Laboratory of Materials Physics, School of Physics and Engineering, Zhengzhou University, Zhengzhou 450001, China

^f Zhixin High School, Guangzhou, 510080, P.R. China.

DFT Calculations

All the calculations were performed based on spin-polarized periodic density functional theory (DFT) implemented in Gaussian 09W.¹ The calculation basis set was B3LYP and the total energy convergence was set to be lower than 10^{-5} eV, and the force convergence was set to be smaller than 0.02 eV/Å. The crystal plane of V_2O_5 for DFT calculation is (001) facet and the crystal plane of C for DFT calculation is (001) facet (JCPDS no. #65-0131 for V_2O_5 and JCPDS no. #26-1080 for C).

Supporting Figures

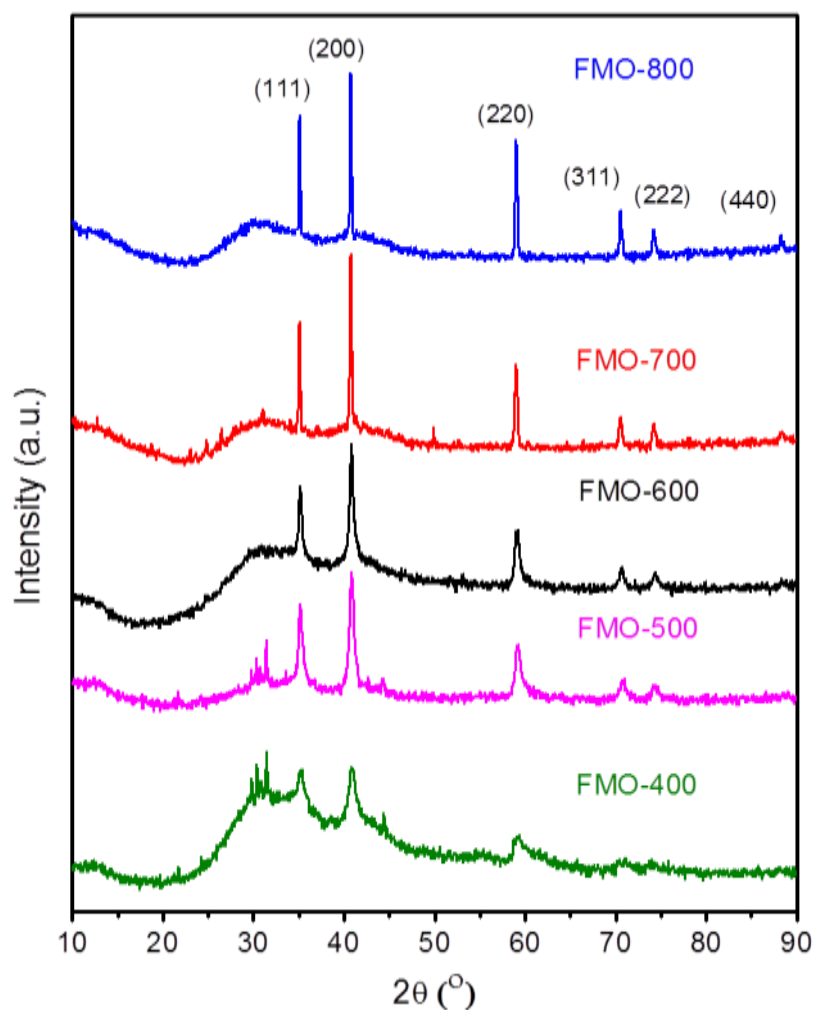


Figure S1. XRD patterns of the FMO samples at different annealing temperature from 400 °C to 800 °C.

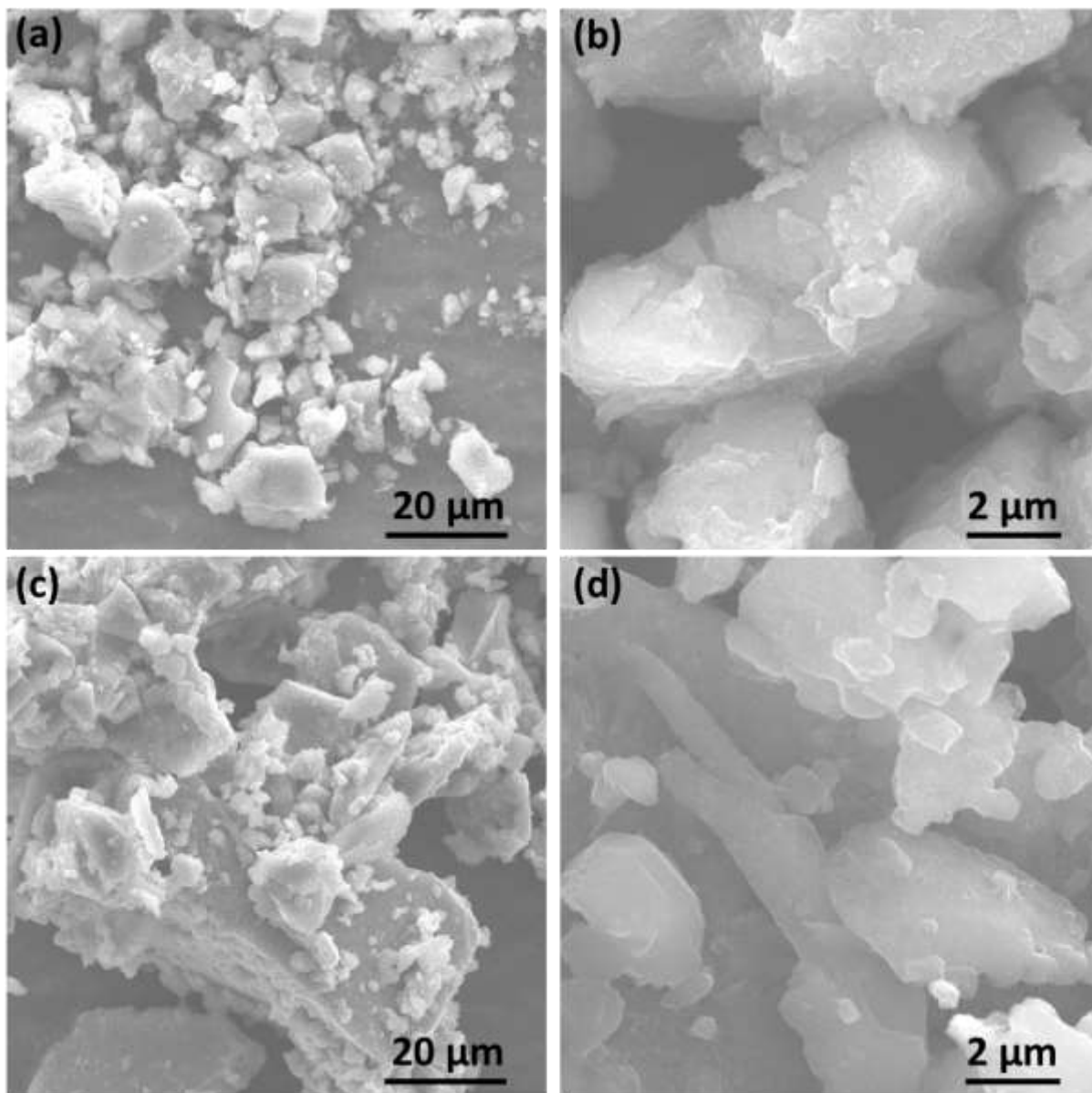


Figure S2. SEM images of (a-b) FMO-400 and (c-d) FMO-500.

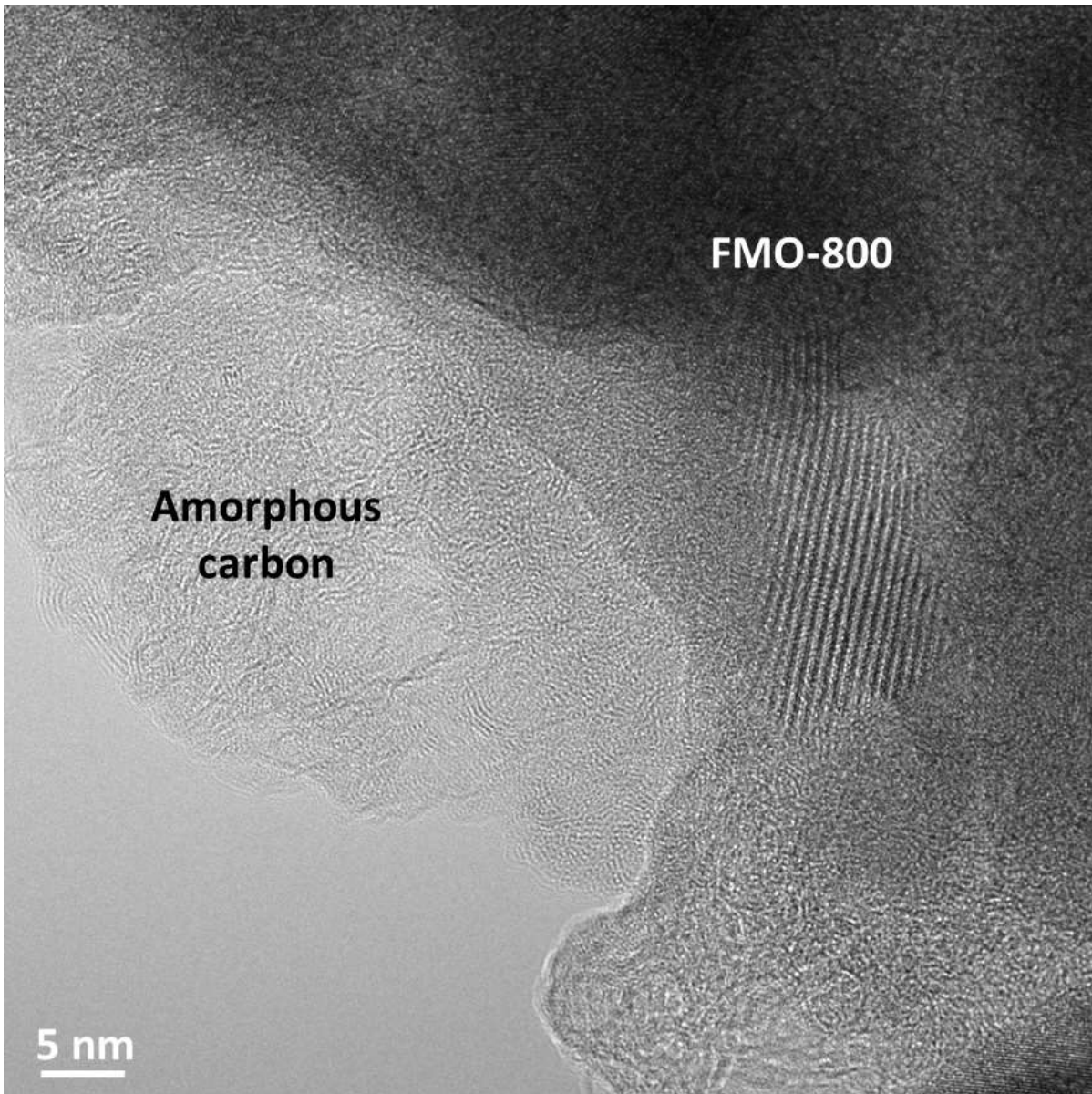


Figure S3. HRTEM of FMO-800 showing the amorphous carbon.

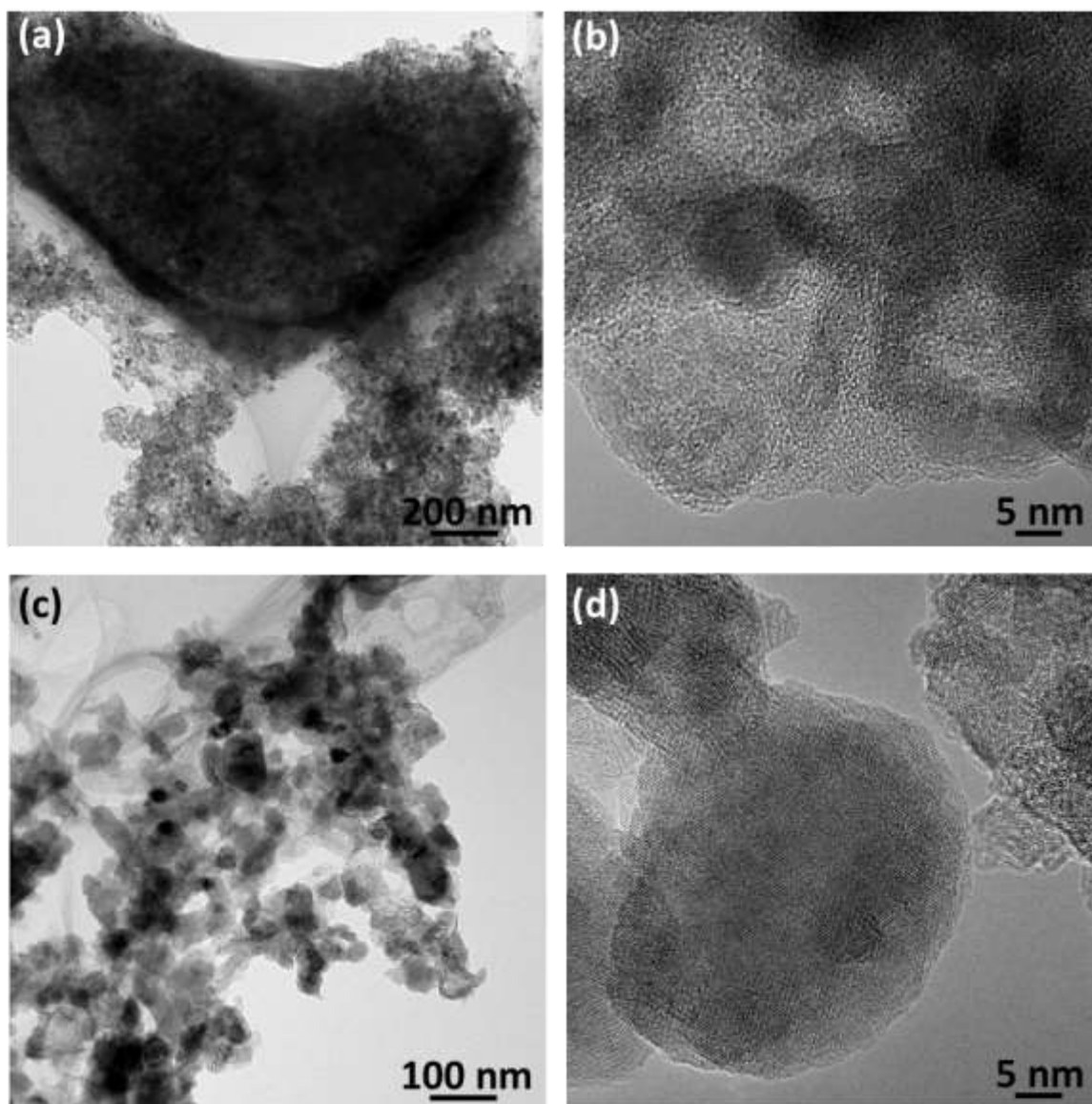


Figure S4. TEM images of (a-b) FMO-600 and (c-d) FMO-700.

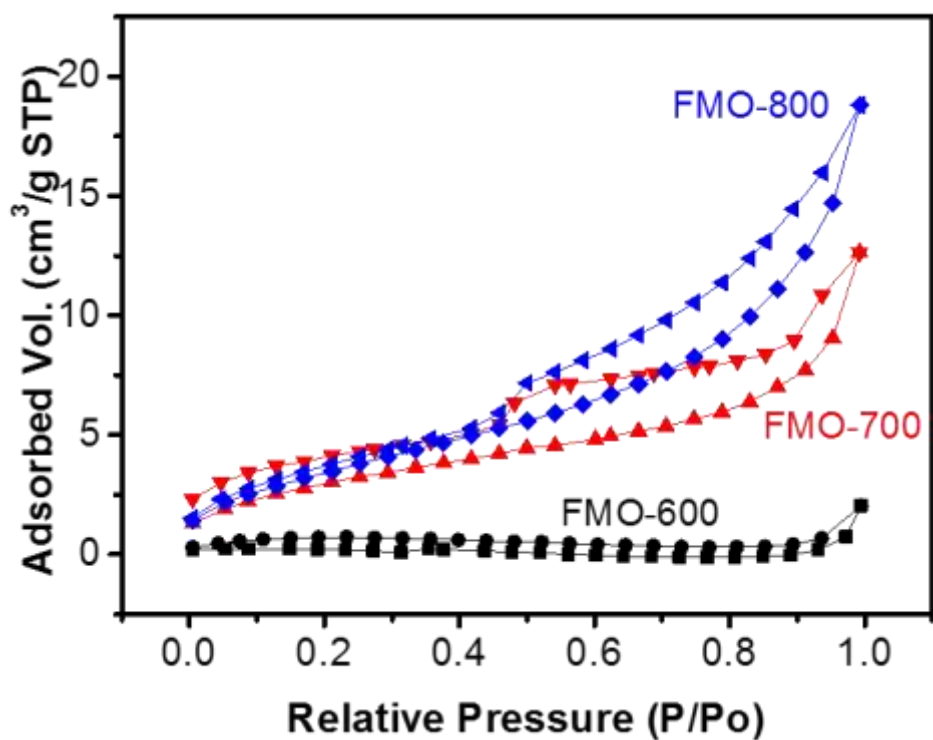


Figure S5. BET surface area of the samples.

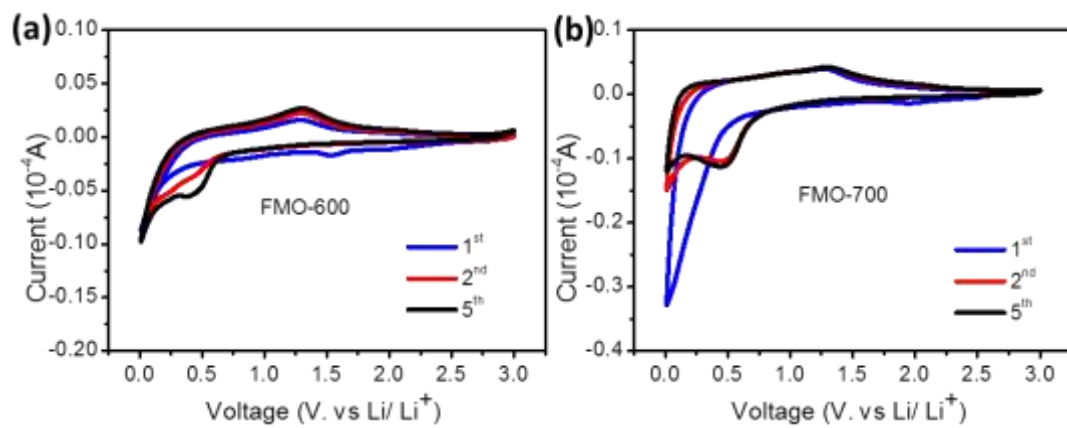


Figure S6. 1st, 2nd and 5th CV curves of (a) FMO-600 and (b) FMO-700.

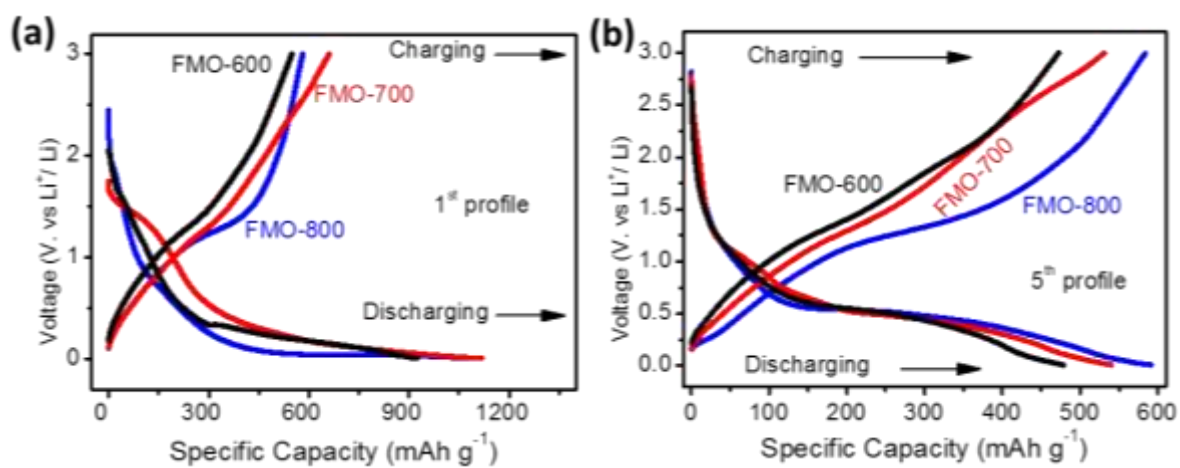


Figure S7. (a) 1st and (b) 5th charge/discharge profiles of the electrodes.

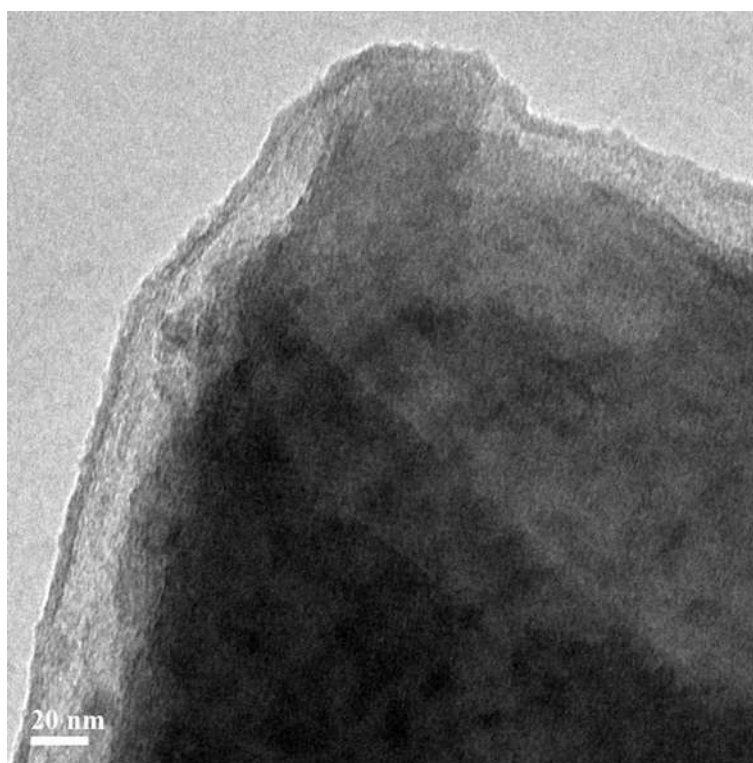


Figure S8. TEM images of FMO-800 after cyclic stability

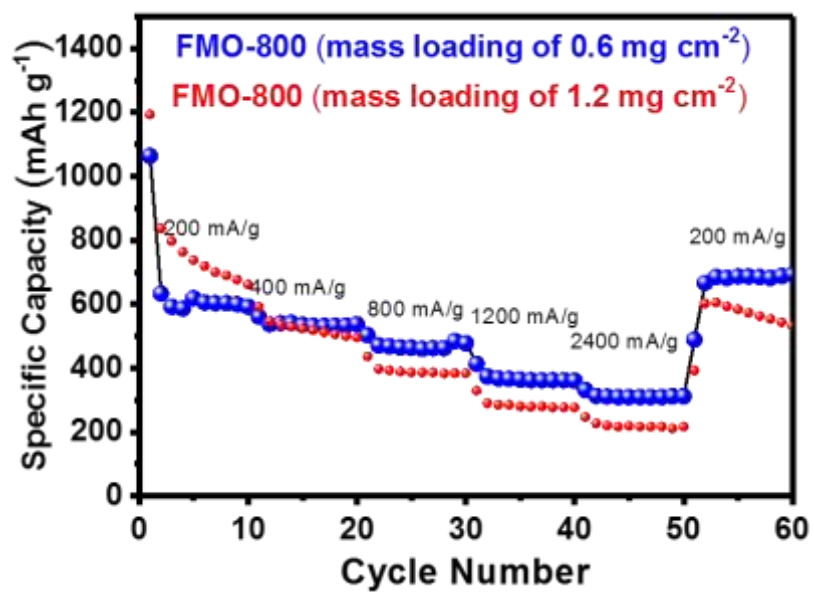


Figure S9. Rate performance of FMO-800 at different mass loading of 0.6 and 1.2 mg cm⁻².

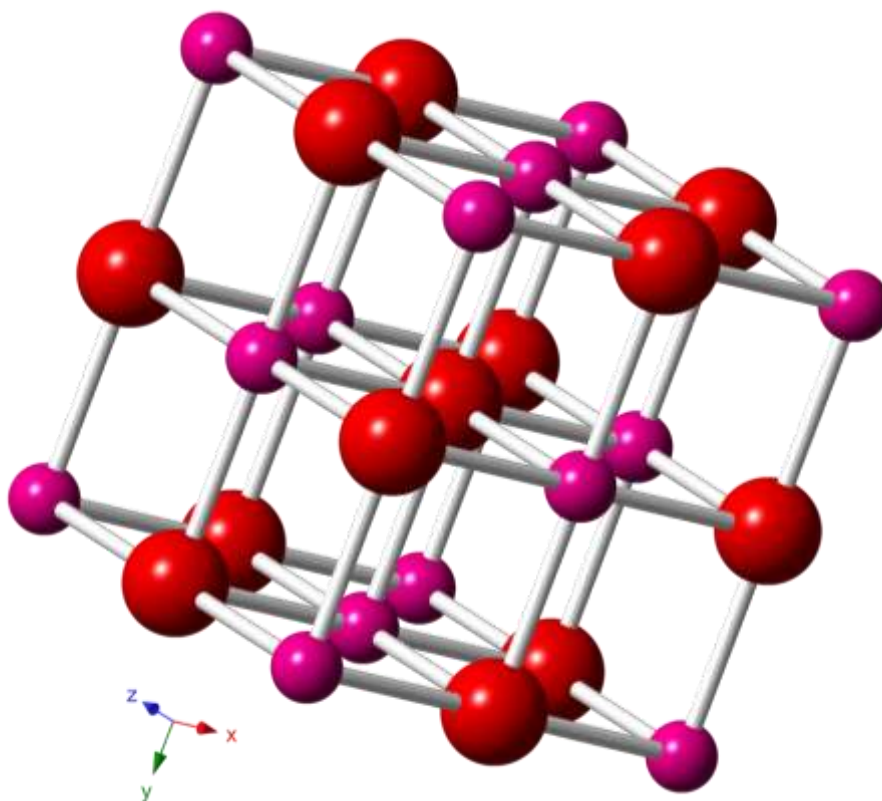


Figure S10. Optimum cluster structure of FMO-600.

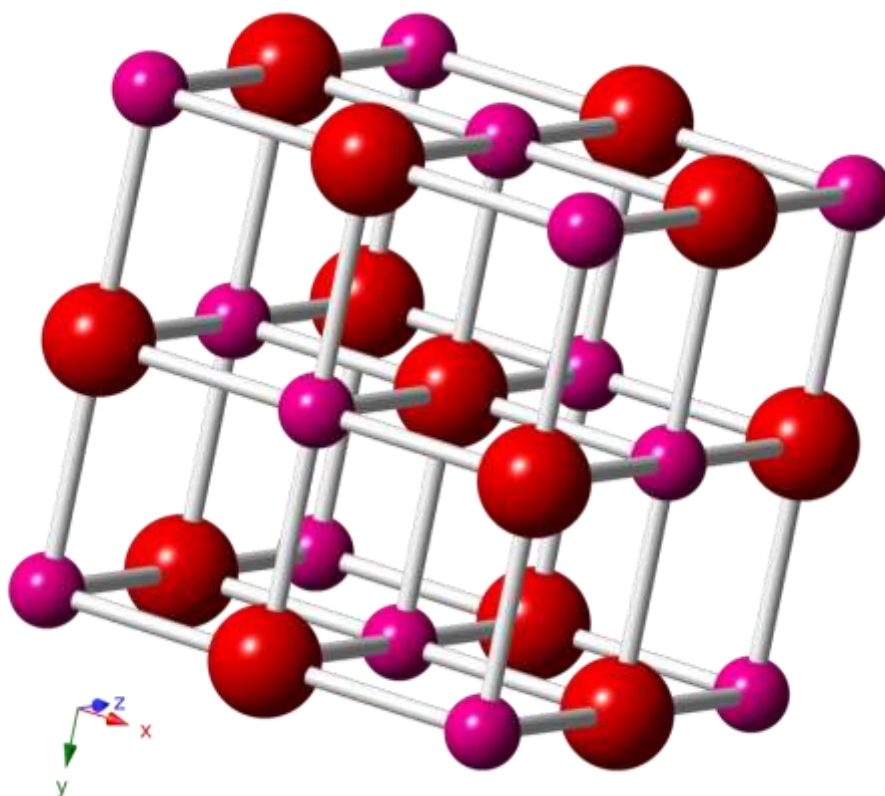


Figure S11. Optimum cluster structure of FMO-700/800.

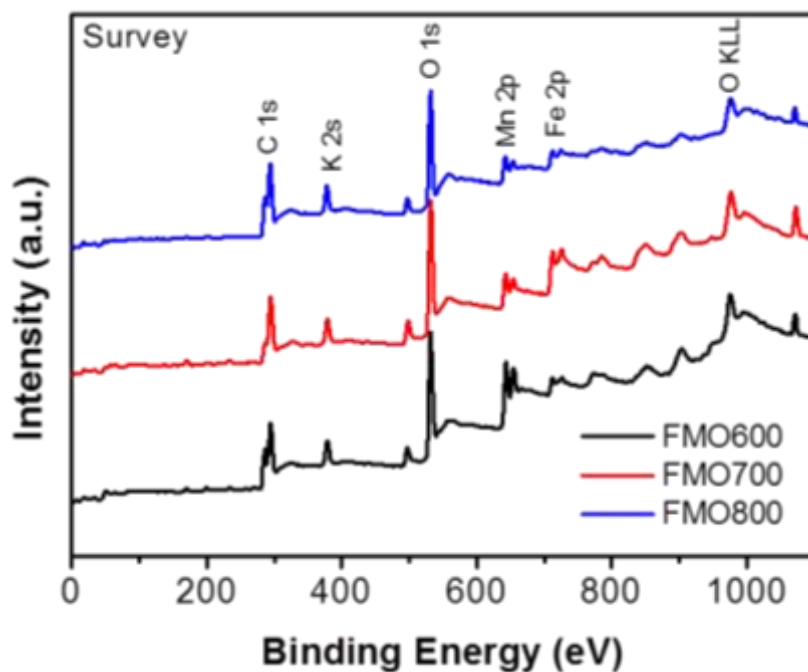


Figure S12. XPS survey spectra of the samples.

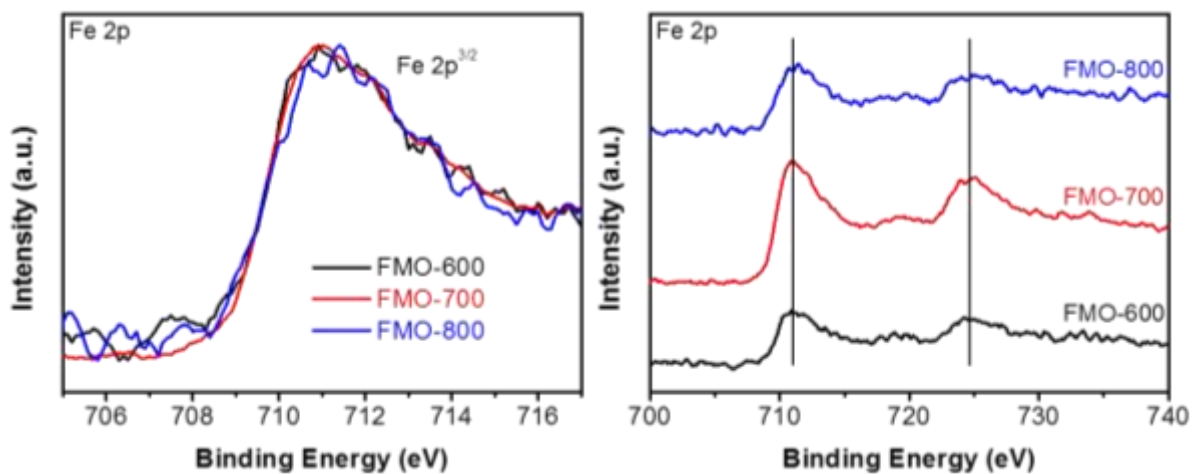


Figure S13. Fe 2p XPS survey spectra of the samples.

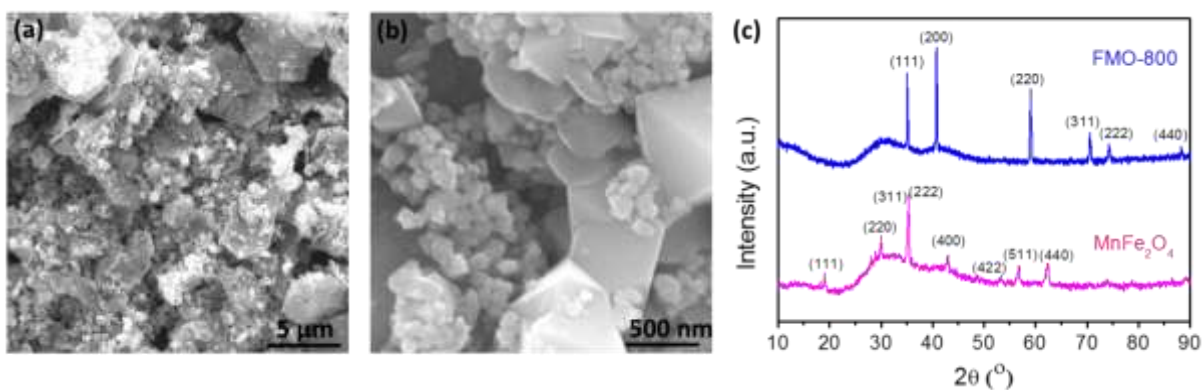


Figure S14. (a-b) SEM images of MnFe₂O₄. (c) XRD spectra of FMO-800 and MnFe₂O₄.

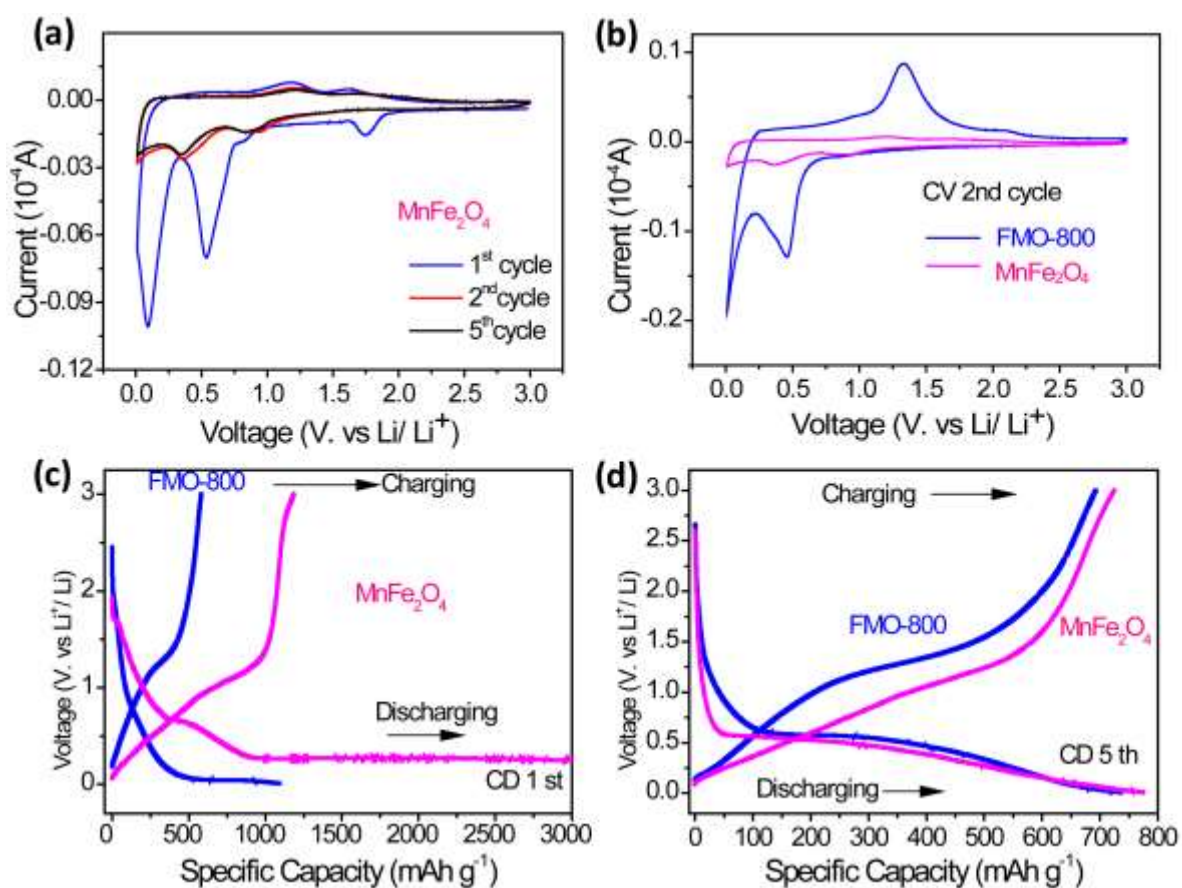


Figure S15. (a) 1st, 2nd and 5th CV curves of MnFe₂O₄. (b) 2nd cycle CV curves of FMO-800 and MnFe₂O₄. (c) 1st and (d) 5th charge/discharge profiles of FMO-800 and MnFe₂O₄.

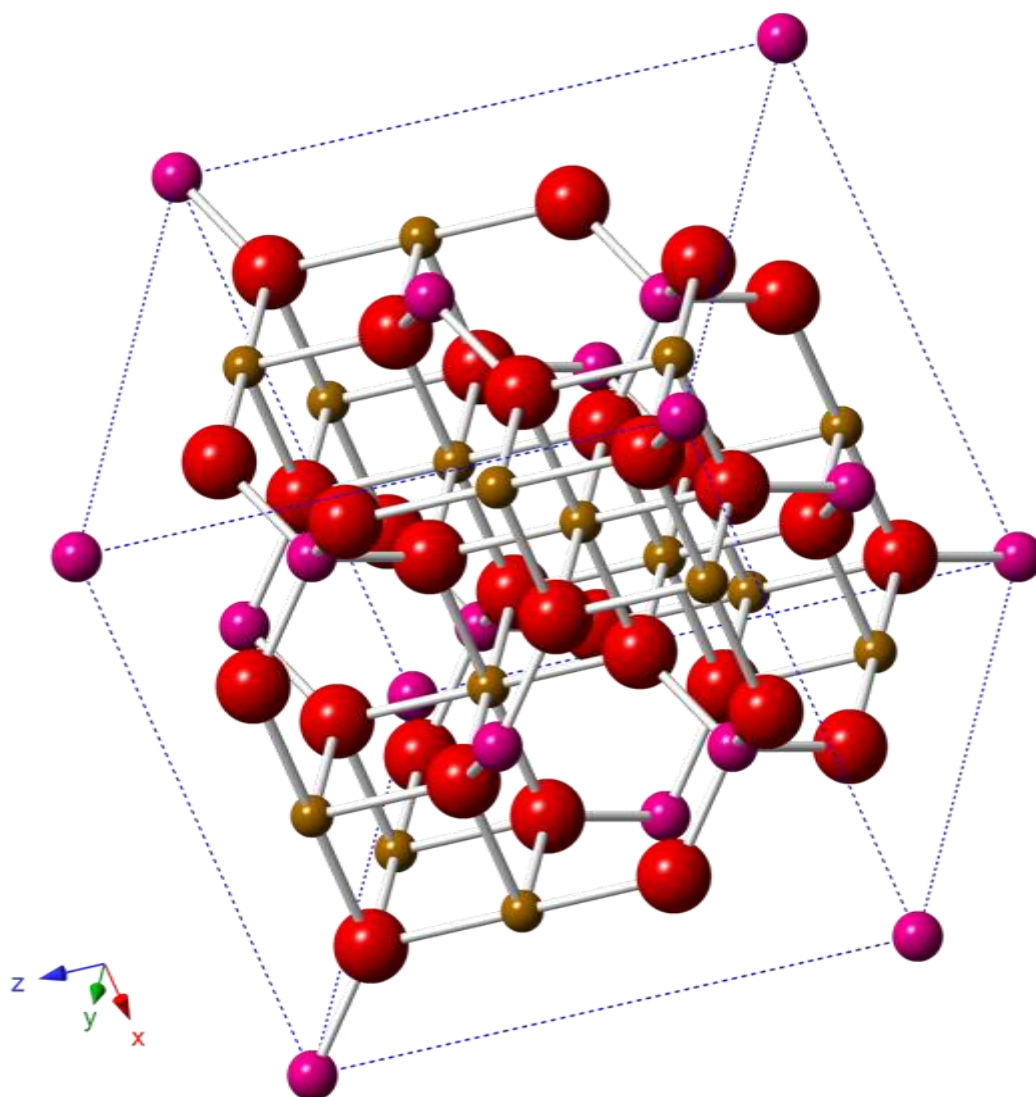


Figure S16. Optimum cluster structure of MnFe_2O_4 .

References

1. M. J. Frisch, G. W. Trucks, H. B. Schlegel, G. E. Scuseria, M. A. Robb, J. R. Cheeseman, J. A. Montgomery, Jr., T. Vreven, K. N. Kudin, J. C. Burant, J. M. Millam, S. S. Iyengar, J. Tomasi, V. Barone, B. Mennucci, M. Cossi, G.; Rega, N. Scalmani, G. A. Petersson, H. Nakatsuji, M. Hada, M. Ehara, K. Toyota, R. Fukuda, J. Hasegawa, M. Ishida, T. Nakajima, Y. Honda, O. Kitao, H. Nakai, M. Klene, X. Li, , J. E. Knox H. P. Hratchian, J. B. Cross, C. Adamo, J. Jaramillo, R. Gomperts, R. E. Stratmann, O. Yazyev, A. J. Austin, R. Cammi, C. Pomelli, J. W. Ochterski, P. Y. Ayala, K. Morokuma, G. A. Voth, P.

Salvador, J. J. Dannenberg, V. G. Zakrzewski, S. Dapprich, A. D. Daniels, M. C. Strain, O. Farkas, D. K. Malick, A. D. Rabuck, K. Raghavachari, J. B. Foresman, J. V. Ortiz, Q. Cui, A. G. Baboul, S. Clifford, , J. Cioslowski B. B. Stefanov, G. Liu, A. Liashenko, P. Piskorz, I. Komaromi, R. L. Martin, D. J. Fox, T. Keith, M. A. Al-Laham, C. Y. Peng, A. Nanayakkara, M. Challacombe, P. M. W. Gill, B. Johnson, W. Chen, M. W. Wong, C. Gonzalez, J. A. Pople, Gaussian, Inc., Pittsburgh PA, **2009**.